Interface Tracking and Multi-Fluid Simulations of Bubbly Flows in Bubble Columns

Akio Tomiyama and Kosuke Hayashi
Kobe University

CFD2011
June 21 – 23, 2011, Trondheim, Norway

Numerical Methods for Bubbly Flow Simulation

Interface Tracking Method (ITM)

$d > 10\Delta x$

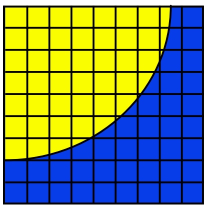

Bubble Tracking Method (BTM)

$d \cong \Delta x$

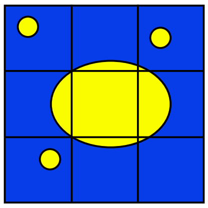

Two-Fluid Model (TFM)

$d < \Delta x$

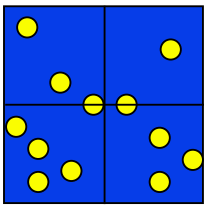

Multi-Fluid Model (MFM)

$d_m < \Delta x$

$(m = 1, \cdots, N)$

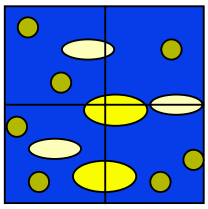

Hybrid CMFD (Computational Multi-Fluid Dynamics)

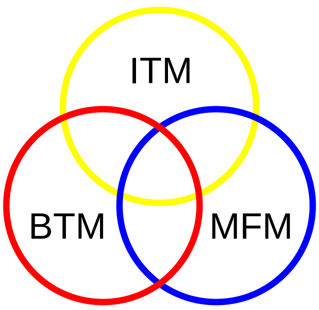

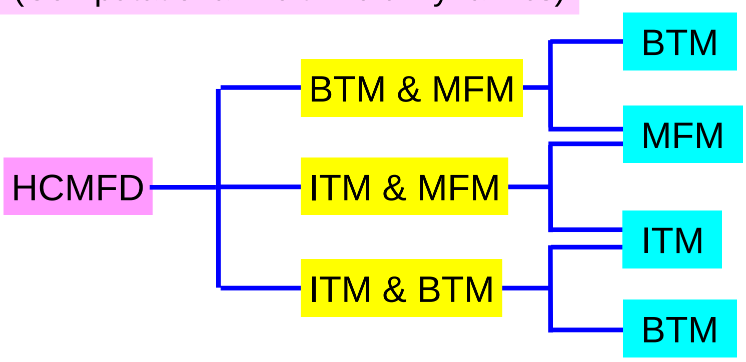

Arbitrary Combination of Different Functions

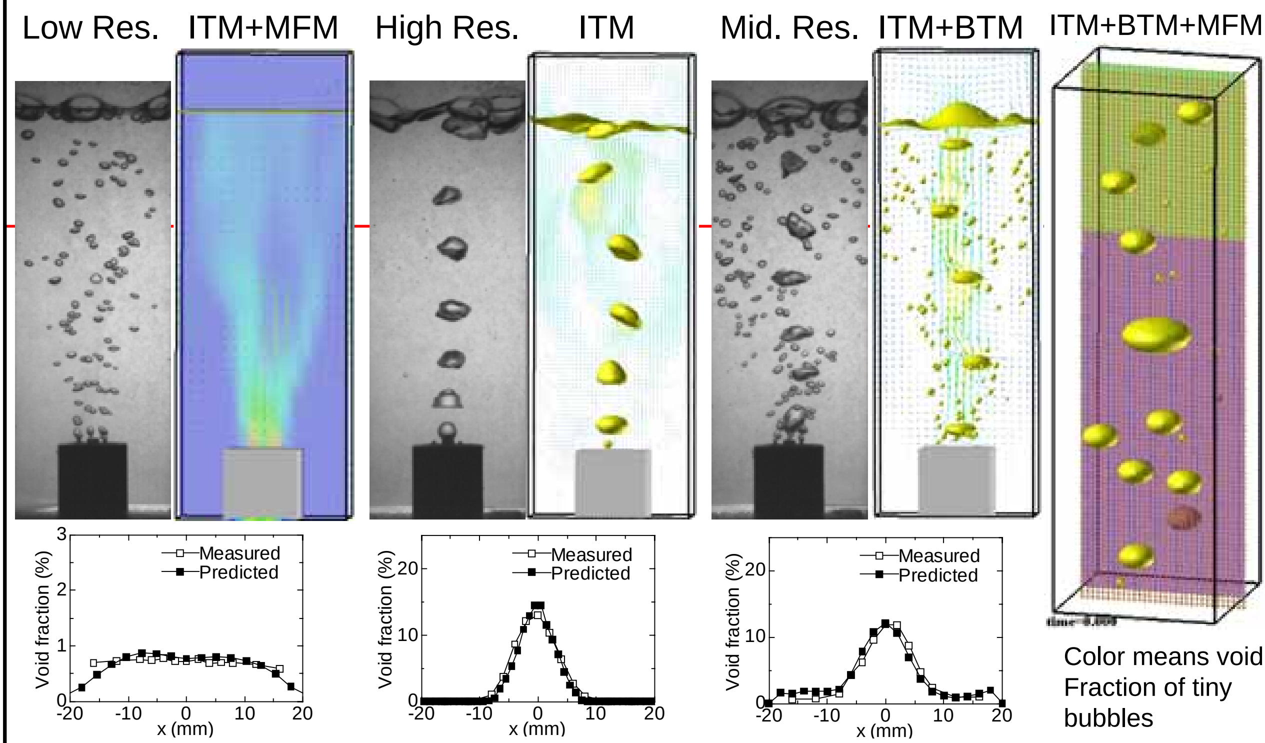

Color means void Fraction of tiny bubbles

Good predictions by using an appropriate combination!

Examples of Interface Tracking Simulations

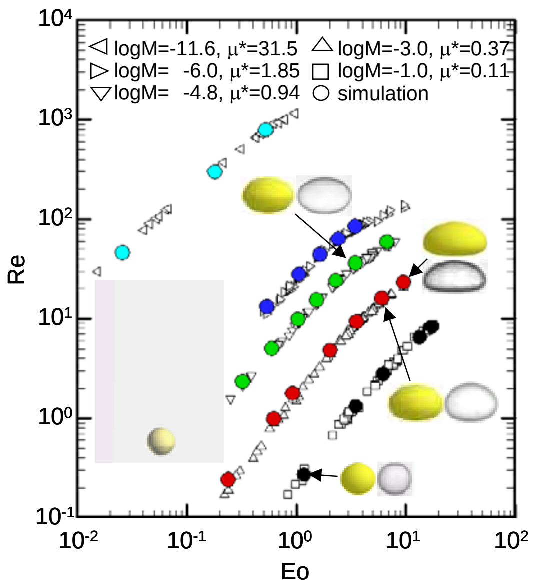

Comparison between measured and predicted drop Re numbers

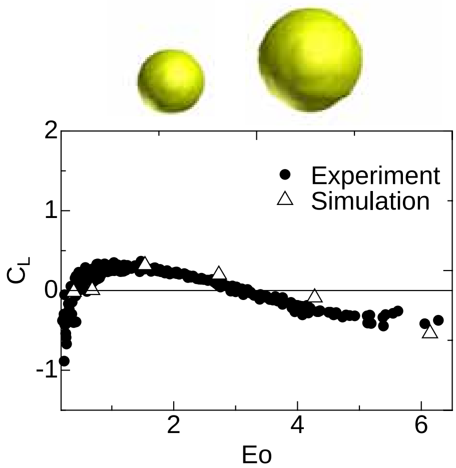

Comparison between measured & predicted bubble lift coefficients

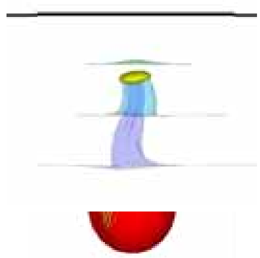

Mixing by Ω-shaped wake

When applying ITM to elementary phenomena in bubble columns, functions for simulating mass transfer, chemical reaction etc. are desired.

Interface Tracking Simulation of Mass Transfer through or onto Gas-Liquid Interface

Mass Transfer through bubbles at high Reynolds numbers

Adsorption and Desorption of Surfactant

Interface Tracking Methods for Mass Transfer

Boundary-Fiited Coordinate Method

Ponoth & McLaughlin, 2000
Sugiyama et al., 2003

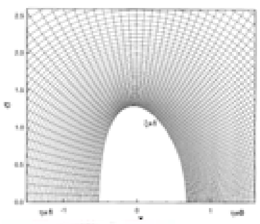

Ponoth & McLaughlin

Front Tracking Method

Koynov et al., 2005, 2006
Tryggvason et al., 2010
Darmana et al., 2007

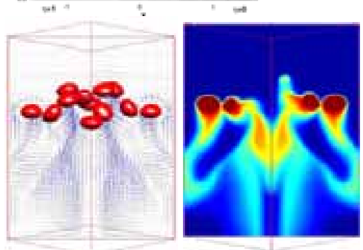

Darmana

Volume of Fluid and Level Set Methods

VOF: Davidson & Rudman, 2002
Bothe et al., 2004, 2010, 2011
Onea et al., 2006, 2009

LS: Yang & Mao, 2005
Wang et al., 2006

Bothe

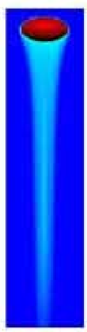

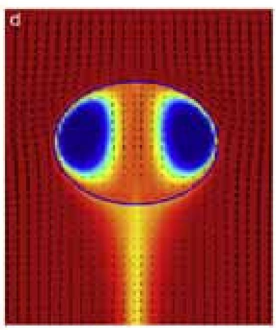

Yang & Mao

Few methods can deal with volume change and bubbles at high Sc and high Re.

Bubbles at High Re and Sc Numbers

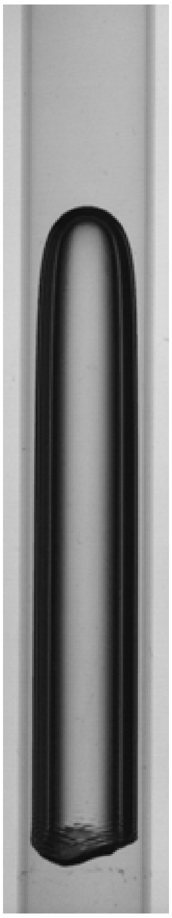

CO_2 bubble in downward water flow

Schmidt number: 530
Reynolds number: 1500
Pipe diameter: 12.5mm

Initial bubble diameter: 29.0 mm
Initial Ingredients: CO_2 only

Final bubble diameter: 7.5 mm
Final ingredients: N_2 (80%), O_2 (20%)

Requirements for simulating bubbles at high Re and Sc numbers

(1) Accurate conservation of species moles

(2) Accurate evaluation of interfacial mass transfer

(3) To capture a thin concentration boundary layer at high Sc

Field Equations

Mass & Momentum Equations (One-Fluid Formulation)

$$\frac{\partial \rho}{\partial t} + \nabla \cdot \rho \boldsymbol{V} = 0$$

$$\frac{\partial \boldsymbol{V}}{\partial t} + \boldsymbol{V} \cdot \nabla \boldsymbol{V} = -\frac{1}{\rho}\nabla P + \frac{1}{\rho}\nabla \cdot \mu[\nabla \boldsymbol{V} + (\nabla \boldsymbol{V})^T] + \boldsymbol{g} + \frac{\sigma \kappa \boldsymbol{n} \delta}{\rho}$$

Conservation of Species Molar Concentration C_k

$$\frac{\partial C_k}{\partial t} + \boldsymbol{V} \cdot \nabla C_k = \nabla \cdot D_k \nabla C_k \qquad (k = G, L)$$

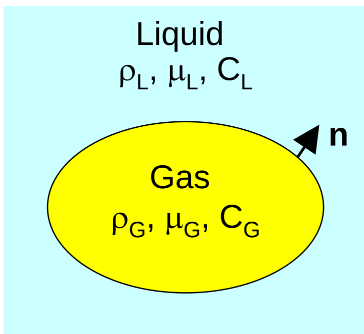

Jump Conditions for C_k

$$C_G = mC_L$$

m: distribution coefficient
(Henry's law)

$$\boldsymbol{j} \cdot \boldsymbol{n}\big|_{int} = -D_G \frac{\partial C_G}{\partial n}\bigg|_{int} = -D_L \frac{\partial C_L}{\partial n}\bigg|_{int}$$

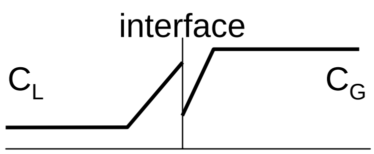

Popular Method: Single-Variable Formulation

Variable Transformation

$$\Phi = \begin{cases} mC_L & \boldsymbol{x} \in L \\ C_G & \boldsymbol{x} \in G \end{cases}$$

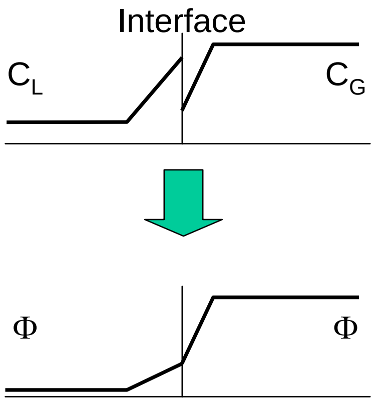

Single-Variable Formulation

$$\frac{\partial \Phi}{\partial t} + \boldsymbol{V} \cdot \nabla \Phi = \nabla \cdot \hat{D} \nabla \Phi$$

$$\Phi\big|_{Gint} = \Phi\big|_{Lint}$$

$$-D_G \frac{\partial \Phi}{\partial n}\bigg|_{int} = -(D_L / m) \frac{\partial \Phi}{\partial n}\bigg|_{int}$$

Solutions, C_L & C_G, are obtained by solving only the single equation for Φ.

This formulation has been often adopted.
(Bothe et al., 2004; Yang & Mao, 2005; Onea et al., 2006; 2009; Francois & Carlson, 2010)

Defect of Single-Variable Formulation

Example: 20mm CO_2 Bubble without Any Mass Transfer (No Volume Change)
Yan & Mao's method (Level set, 5th order WENO, 3rd order TVD, RK)

d=20mm
D=25mm
CO_2-water

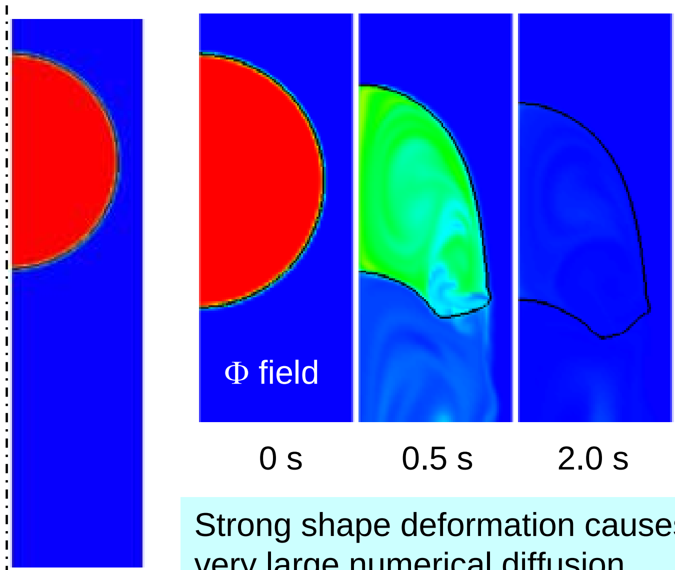

center line

0 s 0.5 s 2.0 s

Strong shape deformation causes very large numerical diffusion

CFD2011: Fleckenstein & Bothe stopped using this for simulating high Re bubbles

Our Method : Two-Variable Formulation

Two-Variable Formulation for Moles, M_G and M_L

$$\frac{\partial M_k}{\partial t} + \int_{S_k} C_k \boldsymbol{V} \cdot d\boldsymbol{S} = \int_{S_k} D_k \nabla C_k \cdot d\boldsymbol{S}$$

$$C_k = \frac{M_k}{\Theta_k}$$

M_k: mole in phase k [mol]

C_k: molar concentration [mol/m^3]

Θ_k: volume of phase k [m^3]

Accurate Advection of M_k

$$M_k^{n+1} = M_k^n - \boxed{\Delta t \int_{S_k} C_k \boldsymbol{V} \cdot d\boldsymbol{S}}$$

Transferred mole = Transferred fluid volume times C

Transferred volume: Volume Tracking Method based on
NSS (Non-uniform Subcell Scheme, Hayashi et al., 2006)
+ EI-LE scheme (Aulisa et al., 2003)

Accurate Conservation of Fluid Volume & Species Moles

Validation: Conservation of Moles

Comparison between single- and two-variable formulations

20 mm CO_2 bubble in water (pipe diameter = 25 mm)

Single-variable (LSM + Φ)

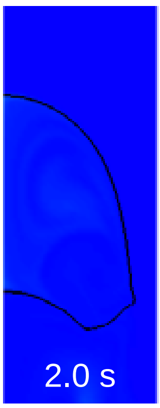

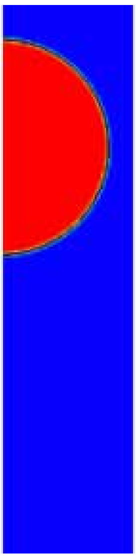

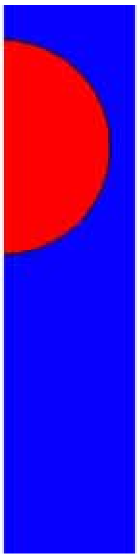

Two-variable (Proposed)

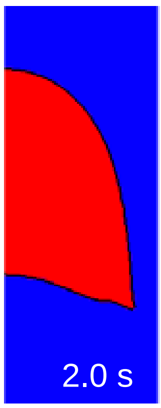

Two-variable formulation gives no numerical diffusion

Computation of Interfacial Mass Transfer

Trend: Use of a Solution based on Boundary Layer Approximation

Tryggvason et al., 2010,   Bothe et al., 2010

$$C_L(\xi,\eta) = \left(\frac{C_{Gi+1j}}{m}\right)\left[1-\mathrm{erf}\left(\frac{\xi}{\sqrt{4D_L\eta/V_B}}\right)\right] \Rightarrow \boldsymbol{j}\cdot\boldsymbol{n}|_{int} = -D_L\left[\frac{\partial C_L}{\partial n}\right]_{int}$$

This may not hold for actual boundary layers (wavy, flow separation, ..).

Evaluation of Interfacial Mass Flux using Single-Variable & Harmonic Mean

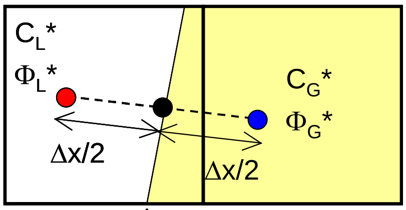

*: interpolated value
Peskin's kernel

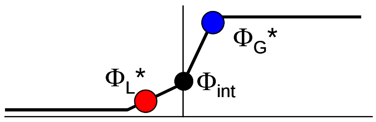

$$\boldsymbol{j}\cdot\boldsymbol{n}|_{int} = -D_G\frac{\Phi_{int}-\Phi_G^*}{\Delta x/2} = -(D_L/m)\frac{\Phi_L^*-\Phi_{int}}{\Delta x/2}$$

Elimination of Φ_{int} ⇒ $\boldsymbol{j}\cdot\boldsymbol{n}|_{int} = -\hat{D}\frac{\Phi_L^*-\Phi_G^*}{\Delta x}$

$$\hat{D} = \frac{2\hat{D}_G\hat{D}_L}{\hat{D}_G+\hat{D}_L} \qquad \hat{D}_k = \begin{cases} D_L/m & \text{for } k=L \\ D_G & \text{for } k=G \end{cases}$$

Validation: Mass Diffusion with Interface Jump

C_G=1 & C_L=0 at t=0
m = 0.2   (C_G=mC_L, C_L>C_G at interface)
D_G/D_L = 10
No volume change
(x, y) = (128, 128 cells)

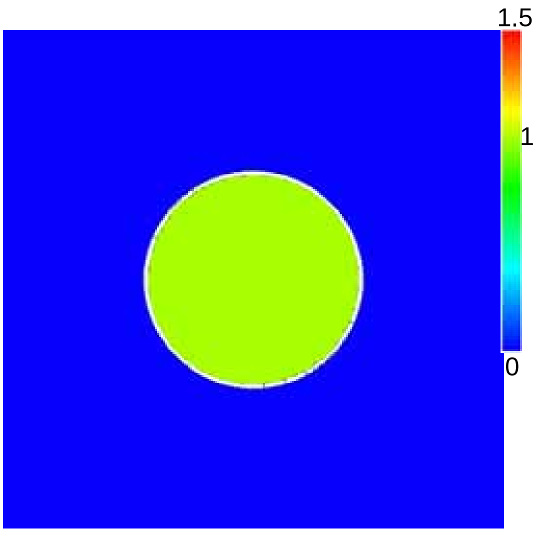

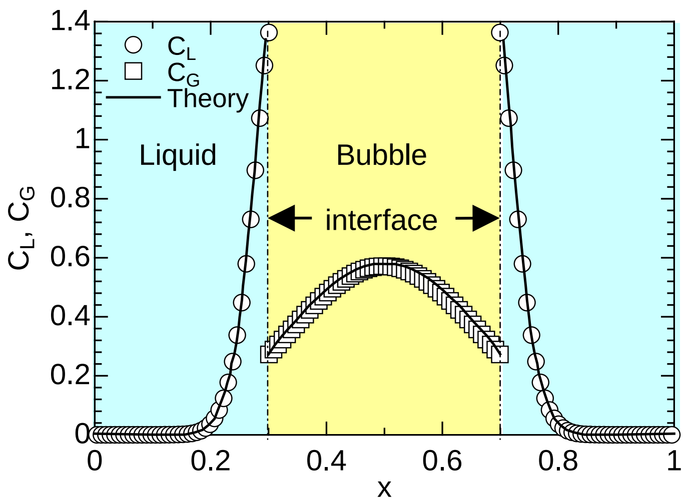

10,000 step

Interfacial mass transfer is accurately computed.

Validation: Mass Transfer from Free Rising Bubble

Case 1: Eo=1, M=1x10^{-4}
Case 2: Eo=40, M=9.2x10^{-3}
Case 3: Eo=3.1, M=5x10^{-7}
Sc=1
m = 1 (no jump in C), C_G=constant
No volume change
(R, H) = (40, 160 cells)

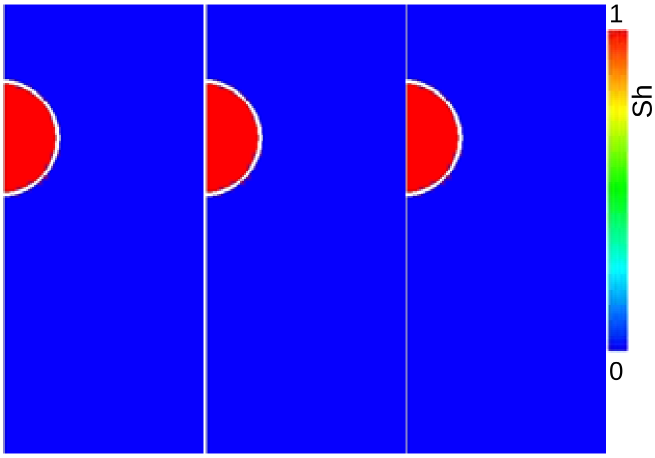

Case 1	Case 2	Case 3
Re=5.5	Re=31	Re=97

Mass transfer coefficient k_L

$$k_L = \frac{1}{A\Delta t}\int_{V\in L}(C_L^{n+1} - C_L^n)dV$$

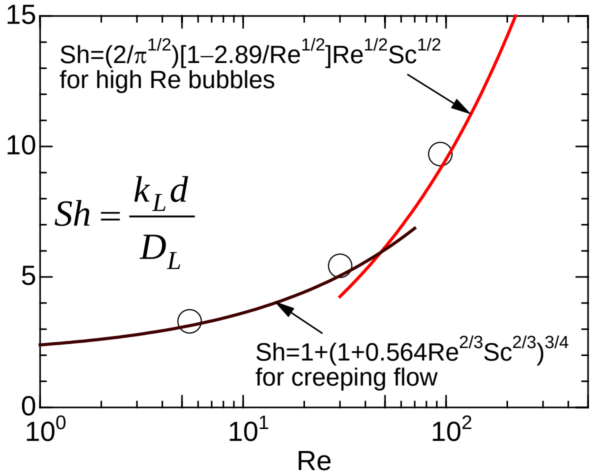

Mass transfer from a bubble at low Re and low Sc is well predicted

Accuracy of Computation of Volume Change

Bubble: d=15 mm, CO_2 100% at t = 0 sec
Pipe: D= 18.6 mm
Re = 2700, Sc = 530
Water: equilibrium concentration of N_2 & O_2
Volume Change : Considered

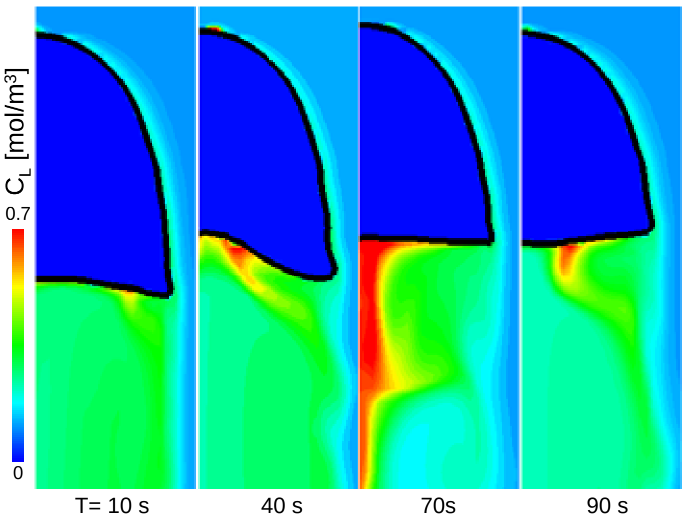

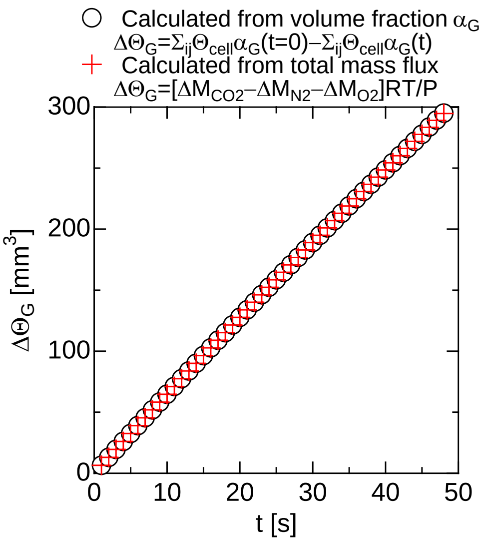

The volume change due to mass transfer is accurately computed.

Simulation of 8 mm CO_2 Bubble in Stagnant Water

Re=1200, Sc=530, D = 18.2 mm

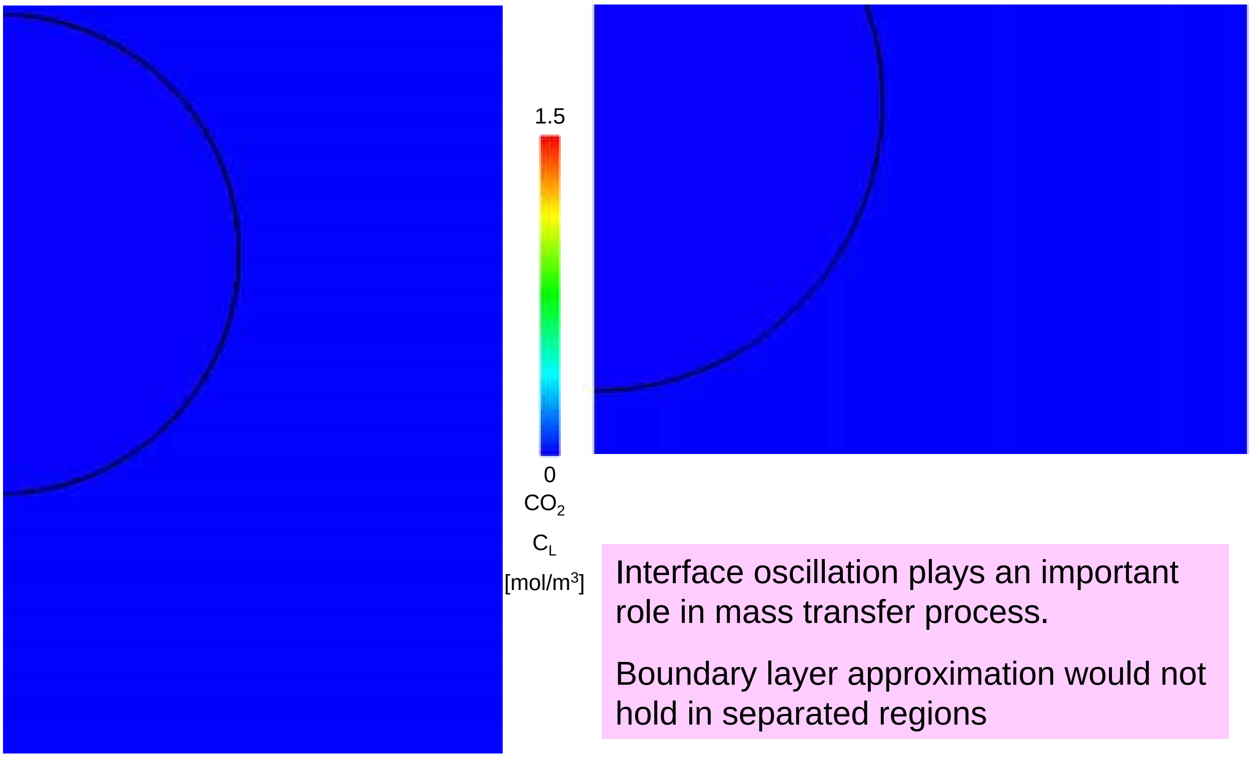

Interface oscillation plays an important role in mass transfer process.

Boundary layer approximation would not hold in separated regions

85 cells for the bubble radius

Comparison with Measured Bubble Dissolution Process

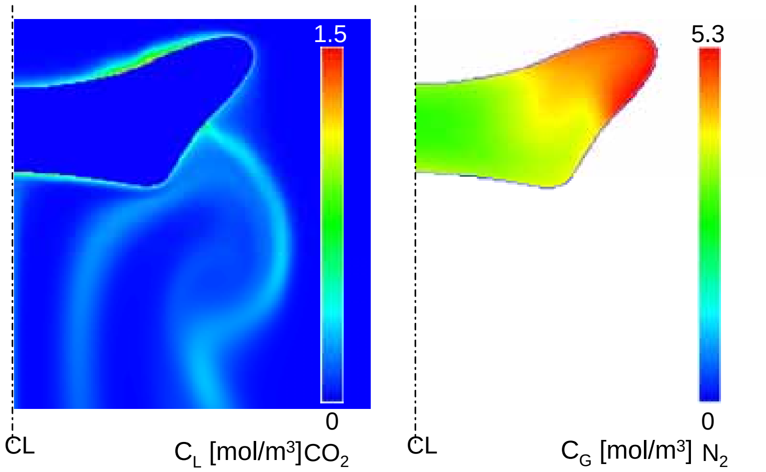

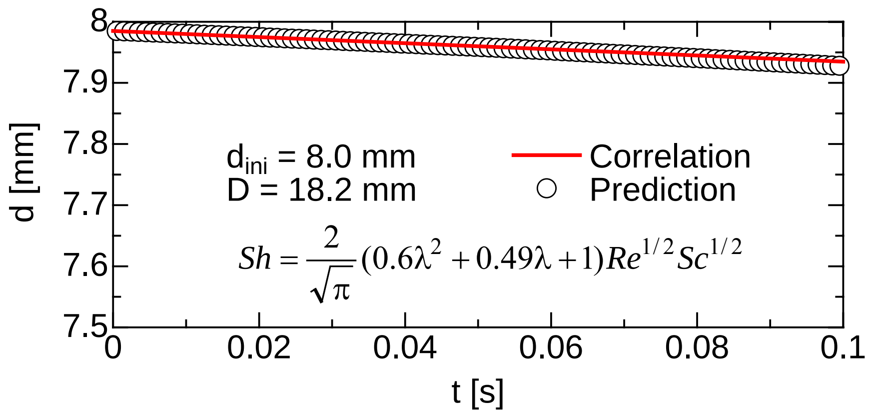

8mm CO_2 Bubble

Cell size = 47 μm
(170 cells for d)

Adaptive Mesh Refinement for Concentration Field

An example of AMR

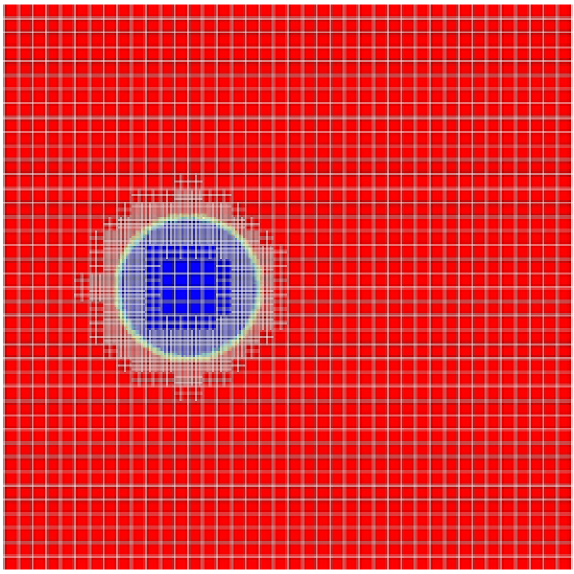

Sc = 500

Reduction of cell numbers 98.4%

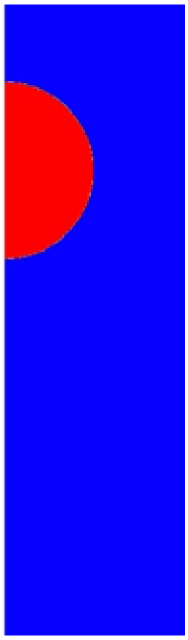

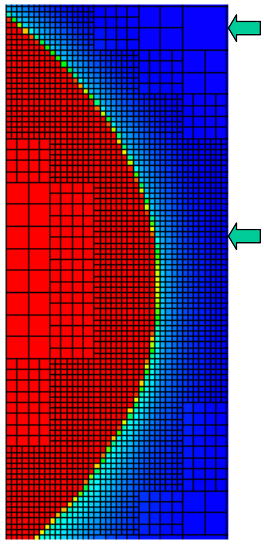

Coarse cell for V and P

Finer cells for Moles near the interface

High Resolution only for Concentration Boundary Layer

Effects of Surfactant on Bubble & Drop Dynamics

1. Reduction of surface tension σ
2. Marangoni effect (tangential force)
3. Increase in damping coefficient of capillary wave

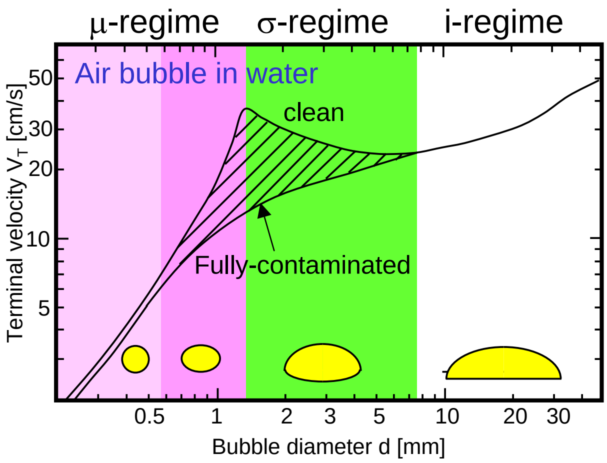

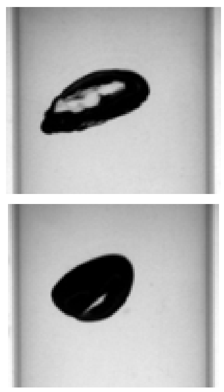

10mm clean bubble

10mm dirty bubble

Decrease in V_T only in some bubble diameter range

Simulations have been performed only for μ-regime

No effects of surfactant on V_T at High Eo_D (Well-known fact)

Increase in V_T at low Eo_D (Almatroushi & Borhan, 2004)

$$Eo_D = \frac{\Delta\rho g D^2}{\sigma}$$

Interface Tracking Methods for Contaminated Bubbles

Boundary-Fiited Coordinate Method

Cuenot et al.,1997 (spherical bubble)

Takagi et al., 2003 (spherical bubble)

Tukovic & Jasak, 2008 (deformed bubble)

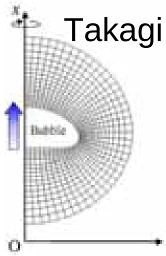

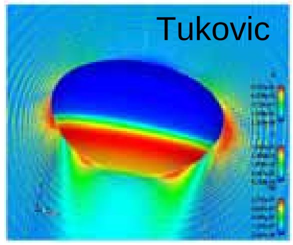

Front Tracking Method

Muradoglu & Tryggvason, 2008

(low Re spheroidal bubble)

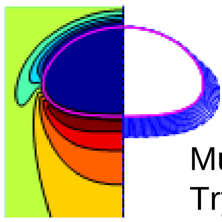

Volume of Fluid and Level Set Methods

VOF: Renardy et al., 2002
James & Lowengrub, 2004
Alke & Bothe, 2009

LS: Xu & Shao, 2003
Xu et al., 2006

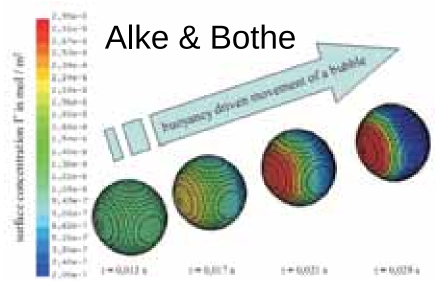

Few methods can simulate highly distorted bubbles at high Re numbers

Field equations & Numerical Methods

Mass & Momentum Equations (Projection Method)

$$\nabla \cdot \boldsymbol{V} = 0$$

$$\frac{\partial \boldsymbol{V}}{\partial t} + \boldsymbol{V} \cdot \nabla \boldsymbol{V} = -\frac{1}{\rho}\nabla P + \frac{1}{\rho}\nabla \cdot \mu[\nabla \boldsymbol{V} + (\nabla \boldsymbol{V})^T] + \boldsymbol{g} + \frac{1}{\rho}[\sigma\kappa\boldsymbol{n} + \nabla_S \sigma]\delta$$

Ghost fluid method

CSF model

Bulk & Surface Concentrations of Surfactant

$$\frac{\partial C}{\partial t} + \mathbf{V} \cdot \nabla C = \nabla \cdot D_B \nabla C + \dot{S}_\Gamma\, \delta$$

Two step method (Muradoglu & Tryggvason)

$$\frac{\partial \Gamma}{\partial t} + \nabla_S \cdot \Gamma \boldsymbol{V}_S = \nabla_S \cdot D_S \nabla_S \Gamma - \dot{S}_\Gamma$$

Extrapolation method (Xu & Zhao)

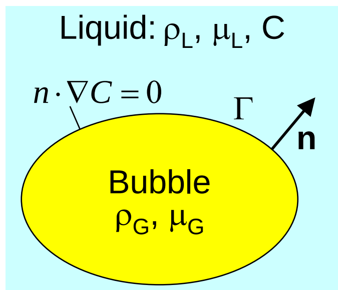

Adsorption-Desorption Kinetics (Langmuir model)

$$\dot{S}_\Gamma = -\boldsymbol{n} \cdot (D_C \nabla C|_{int}) = k[C_S(\Gamma_{max} - \Gamma) - \beta\Gamma]$$

k: adsorption constant
β: desorption constant
(Frumkin & Levich)

Advection of Interface

$$\frac{\partial \phi}{\partial t} + \boldsymbol{V} \cdot \nabla \phi = 0$$

Level set method (Susuman)

Surface Tension

$$\sigma = \sigma_0 + RT\Gamma_{max} \ln\left(1 - \frac{\Gamma}{\Gamma_{max}}\right)$$

Small Air Bubble in Contaminated Water (μ-Regime)

Fluids: air and water

Surfactant:1-pentanol
- k=5.08 $m^3/mol \cdot s$
- β=21.7 mol/m
- Γ_{max}=5.9x10^{-6} mol/m^2

Bubble diameter: 0.6-0.98 mm

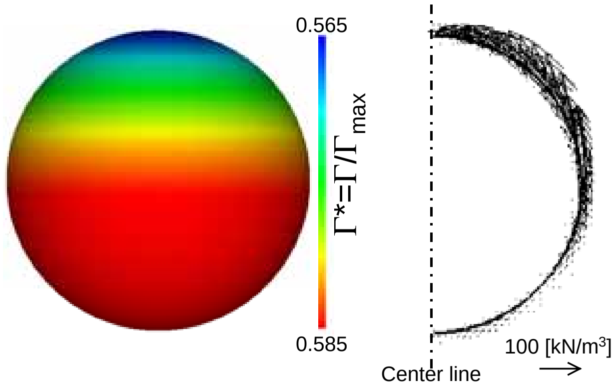

d=0.72mm, C=30mol/m³

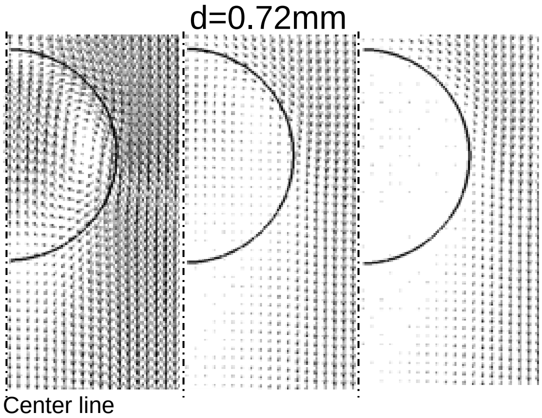

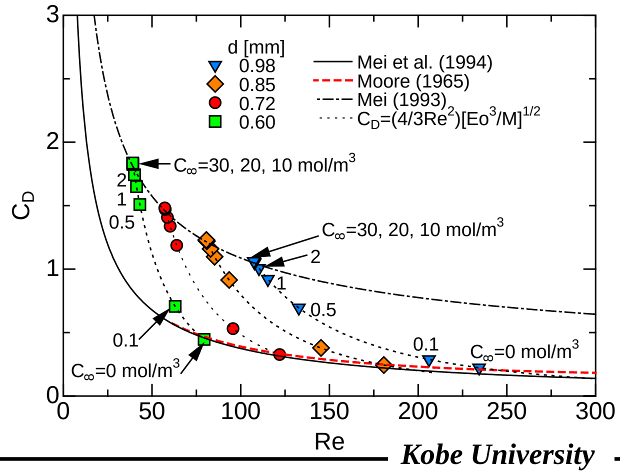

Distorted Air Bubble in Contaminated Water (σ-Regime)

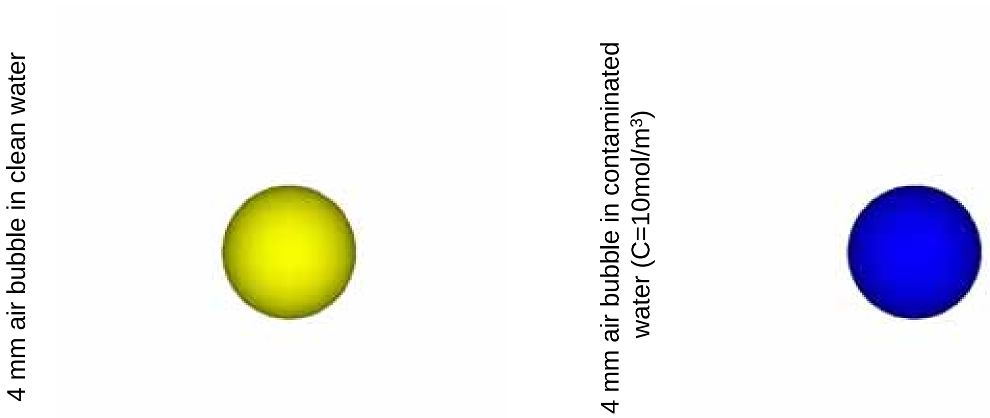

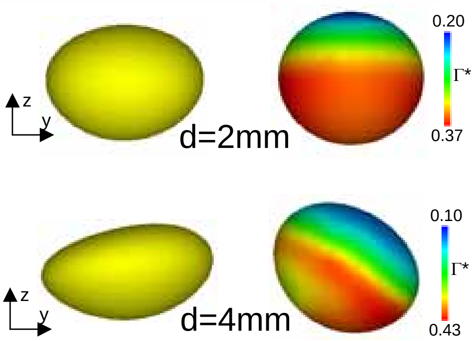

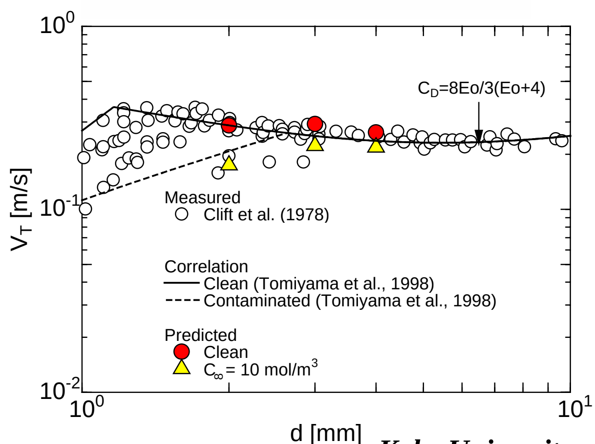

Taylor Bubbles in Air-Water System (σ and i-Regimes)

No effects of surfactant on V_T at High Eo_D (Well-known fact)
Increase in V_T at low Eo_D (Almatroushi & Borhan, 2004)

$$Eo_D = \frac{\Delta\rho g D^2}{\sigma}$$

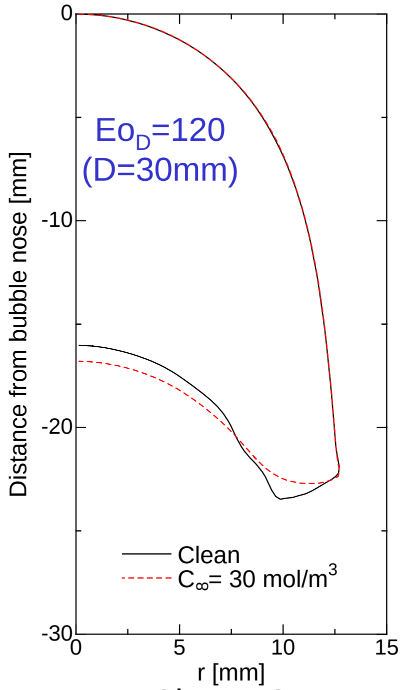

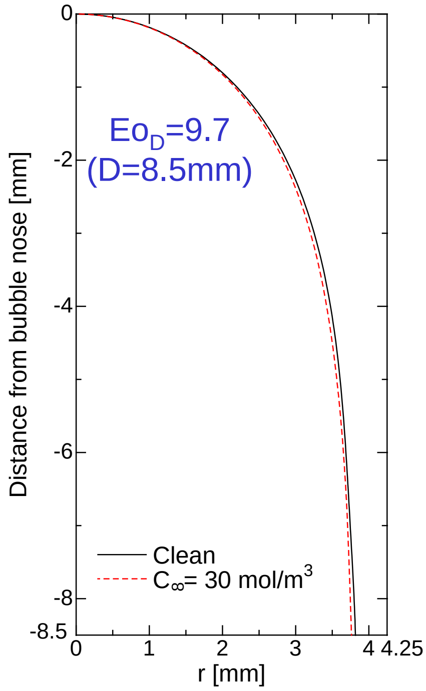

	Clean	Contam.
V_T(m/s)	0.187	0.187

	Clean	Contam.
V_T(m/s)	0.049	0.056

Distributions of Surfactant, Marangoni Force & Velocity

Eo_D=120

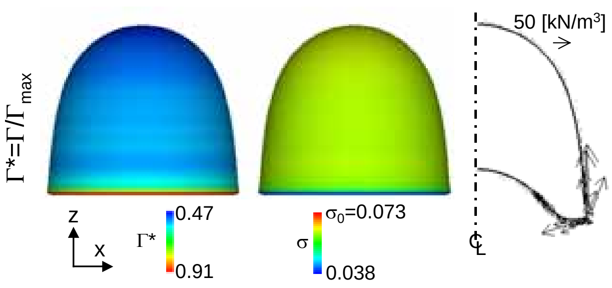

Eo_D=9.7

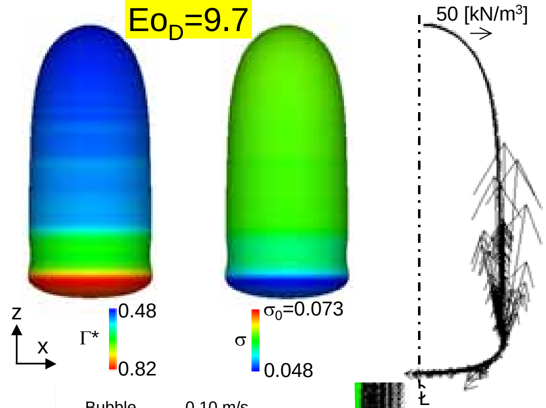

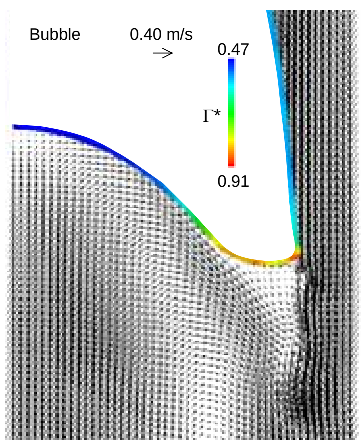

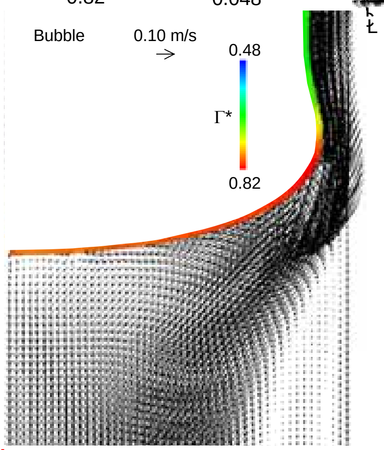

Marangoni force acts only at bottom edge.
Surfactant distribution strongly depends on velocity profile.

Cause of V_T Increase at Low Eo_D

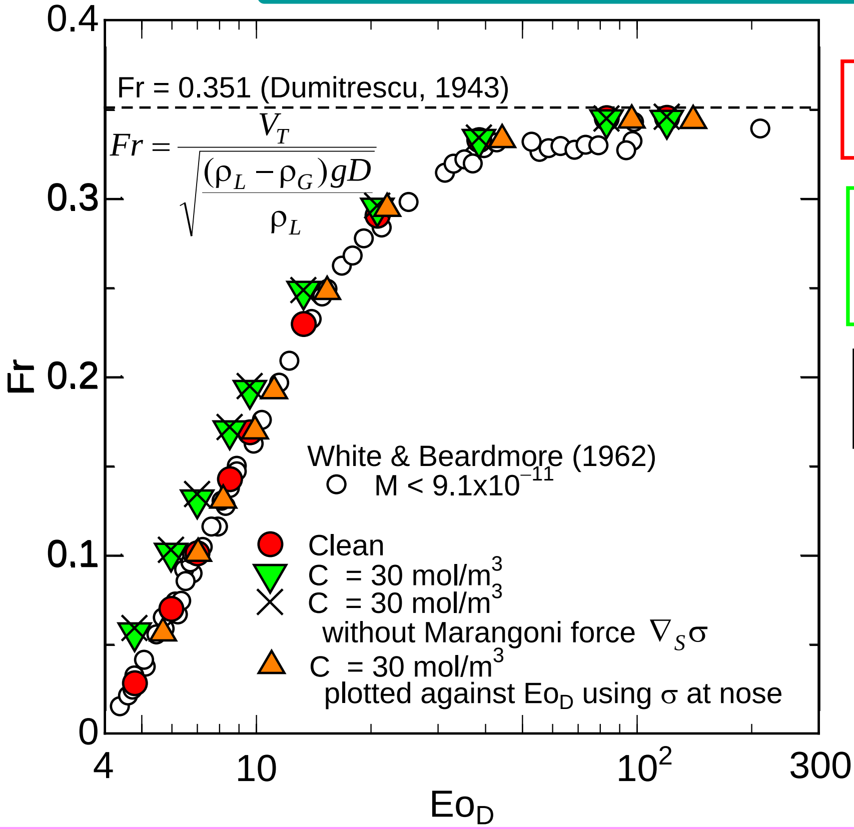

Good predictions for the clean system

Contaminated case
high Fr at low Eo
same Fr at high Eo

Negligible effect of Marangoni force

$$Eo_D = \frac{\Delta \rho g D^2}{\sigma_{nose}}$$

Surface tension at bubble nose is the key parameter

The nose surface tension determines the rise velocity of a low M Taylor Bubble

Multi-Fluid Simulation of Bubbly Flow in a Bubble Column

Validation of Bubble Coalescence and Breakup Model

Effects of Fine Particles on Bubble Coalescence

Closure Relations of MFM for Poly-Dispersed Flow

Dispersed Phases $(m = 0, \cdots, N)$

$$\frac{\partial n_m}{\partial t} + \nabla \cdot n_m \boldsymbol{V}_m = \sum_{m' \neq m} (\Gamma_{m' \to m} - \Gamma_{m \to m'}) - R_m$$

$$\alpha_m \rho_G \frac{D\boldsymbol{V}_m}{Dt} = -\nabla P + \boldsymbol{g} - \left(\boldsymbol{M}_{int\,m} + \boldsymbol{M}_{\Gamma_m} + \boldsymbol{M}_{Rm} \right)$$

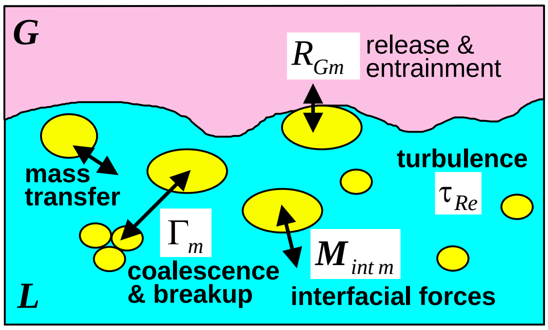

Continuous Gas & Liquid Phases

$$\frac{\partial \alpha_G}{\partial t} + \nabla \cdot (\alpha_G \boldsymbol{V}_C) = \sum_{m=0}^{N} R_m \qquad \frac{\partial \alpha_L}{\partial t} + \nabla \cdot (\alpha_L \boldsymbol{V}_C) = 0$$

$$\alpha_C \rho_C \frac{D\boldsymbol{V}_C}{Dt} = -\nabla P + \boldsymbol{F}_S + \alpha_C \rho_C \boldsymbol{g} + \sum_{m=0}^{N} \left(\boldsymbol{M}_{int\,m} + \boldsymbol{M}_{R_m} \right) + \nabla \cdot \alpha_C (\tau + \tau_{Re})$$

Experiments on single bubbles and drops in infinite liquids or in pipes
- ➡ Drag and lift correlations for various bubbles and drops

Experiments on mass transfer from single bubbles in vertical pipes
- ➡ Sherwood number correlations

Experiments on turbulent poly-dispersed bubbly pipe flows
- ➡ Validation of two-phase turbulence model

Experiments on poly-dispersed bubbly flow in a bubble column
- ➡ Validation of bubble coalescence and breakup models

Experimental Setup & Conditions

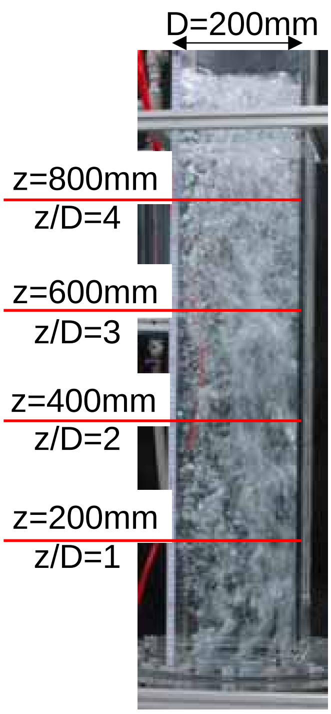

H x W x D : 1400 x 200 x 200 [mm]
Fluids : Air-water at 25 ^{o}C and 1 atm
Gas flow rate : 1.44 x 10^{-3} m^3/s (J_G= 0.036 m/s)
Initial liquid level : 1 m

Void distribution: Conductivity probe
Bubble sizes: Images (2500 bubbles/elevation)

Gas diffusers

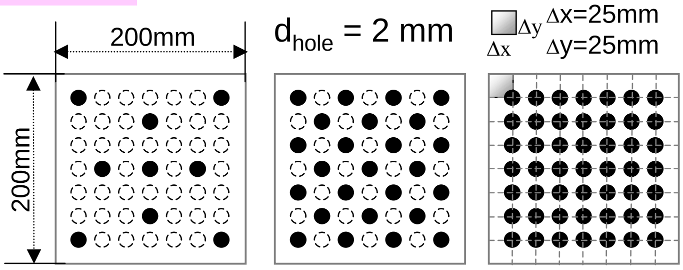

	N_{hole}=9	N_{hole}=25	N_{hole}=49
Q_{hole} [cc/s]	160	57.6	29.4
d_{exp} [mm]	27.3	18.1	13.9

Flow Patterns (High-Speed Video Images)

D=200 mm

z ~ 800 mm

z ~ 200 mm

z ~ 75 mm

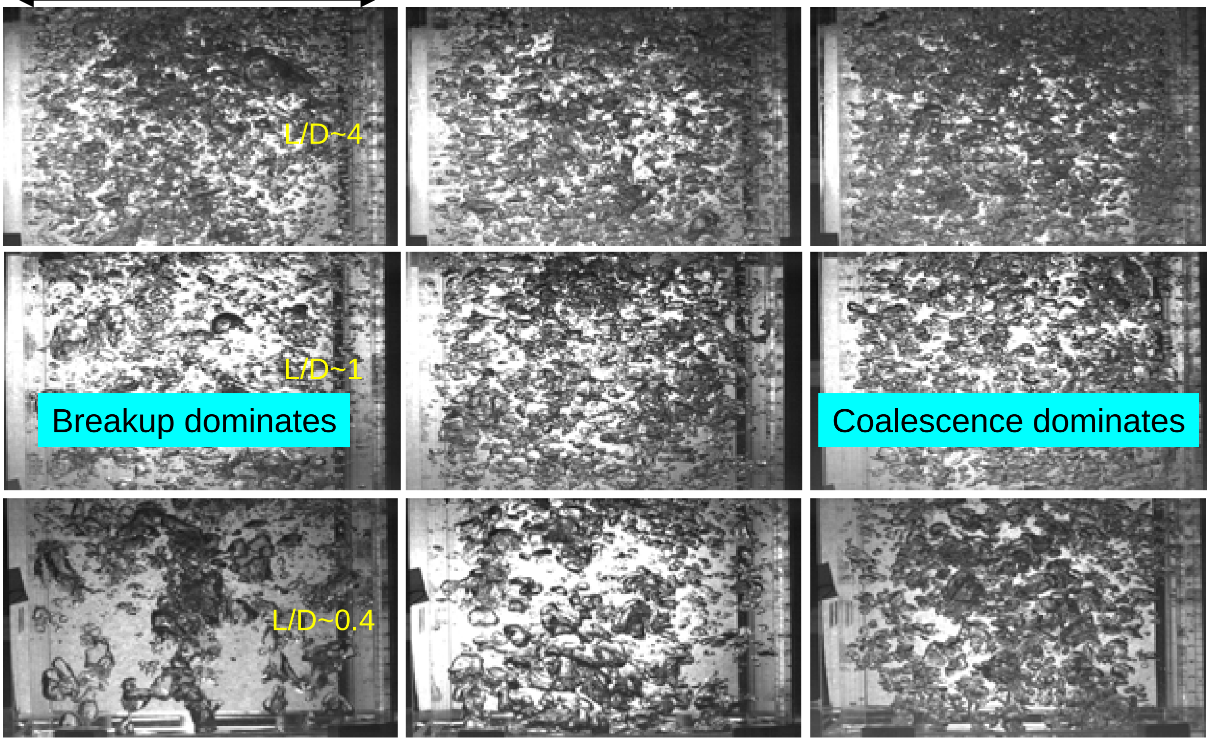

N_{hole}=9, d=27.3mm | N_{hole}=25, d=18.1mm | N_{hole}=49, d=13.9mm

Bubble Coalescence & Breakup Models

$$\frac{\partial n_m}{\partial t} + \nabla \cdot n_m \boldsymbol{V}_m = \sum_{m' \neq m} (\underbrace{\Gamma_{m' \to m}}_{\text{Source}} - \underbrace{\Gamma_{m \to m'}}_{\text{Sink}})$$

Source: $\sum_{m' \neq m} \Gamma_{m' \to m} = \underbrace{\int_{\theta_m}^{\infty} r_B(\theta_m, \theta_{m'}) f(\theta_{m'}) d\theta_{m'}}_{\text{Breakup birth}} + \underbrace{\frac{1}{2} \int_0^{\theta_m} r_C(\theta_{m'}, \theta_m) f(\theta_{m'}) f(\theta_m - \theta_{m'}) d\theta_{m'}}_{\text{Coalescence birth}}$

Sink: $\sum_{m' \neq m} \Gamma_{m \to m'} = \underbrace{\int_0^{\theta_m} \theta_{m'} r_B(\theta_{m'}, \theta_m) d\theta_{m'} \frac{f(\theta_m)}{\theta_m}}_{\text{Breakup death}} + \underbrace{\int_0^{\infty} r_C(\theta_{m'}, \theta_m) f(\theta_{m'}) d\theta_{m'} f(\theta_m)}_{\text{Coalescence death}}$

Breakup | Luo & Svendsen

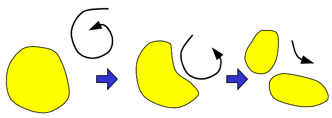

Collision of turbulent eddies

Coalescence

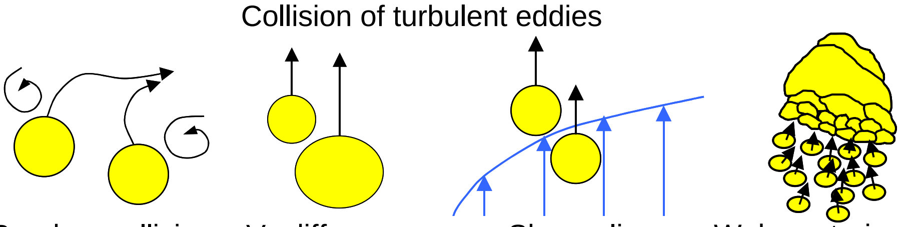

Random collision | V_B difference | Shear slip | Wake entrainment

$\underbrace{\text{Random collision} \quad V_B \text{ difference} \quad \text{Shear slip}}_{\text{Prince \& Blanch}}$ — Wang

Comparison of Bubble Size Distributions

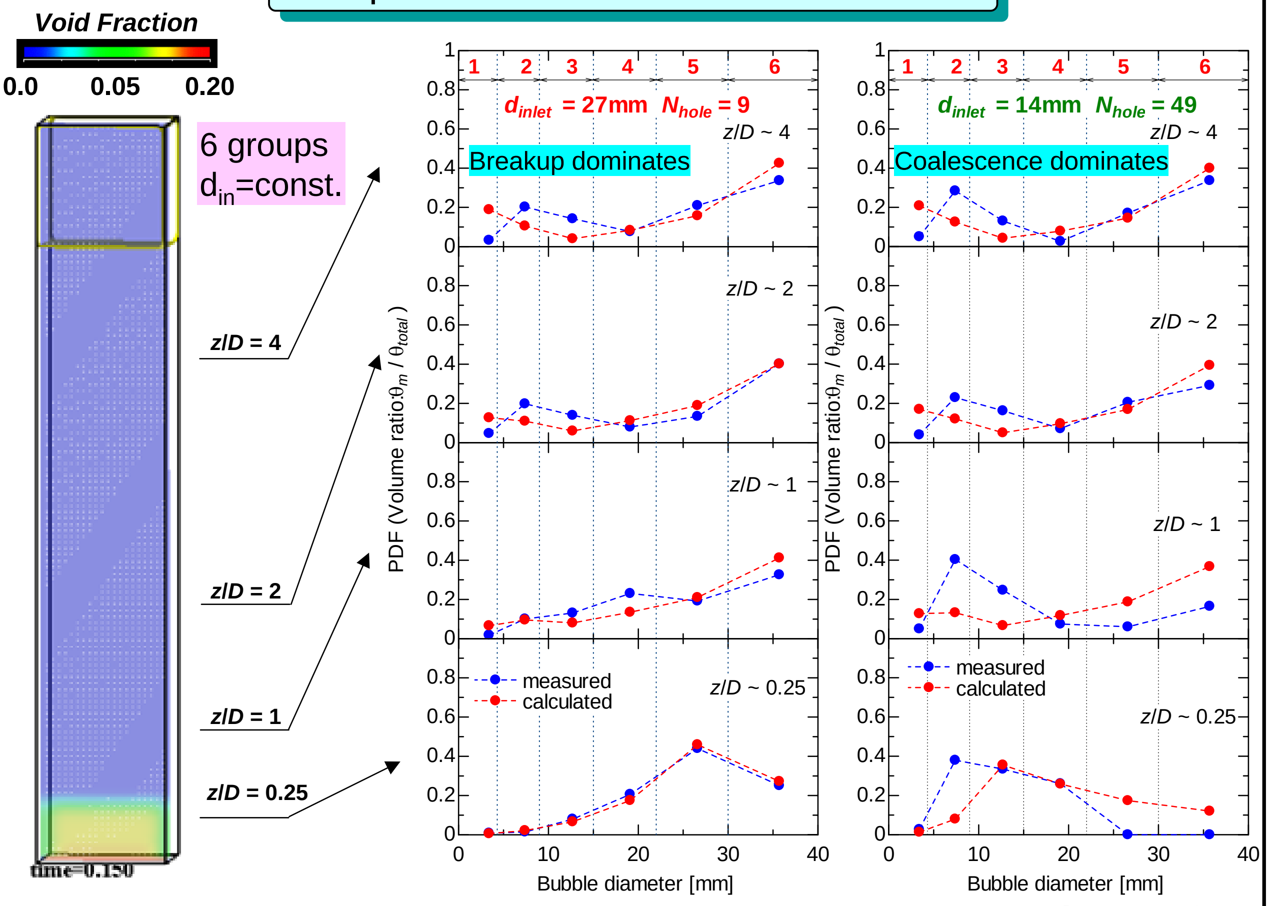

Comparison of Void Distributions

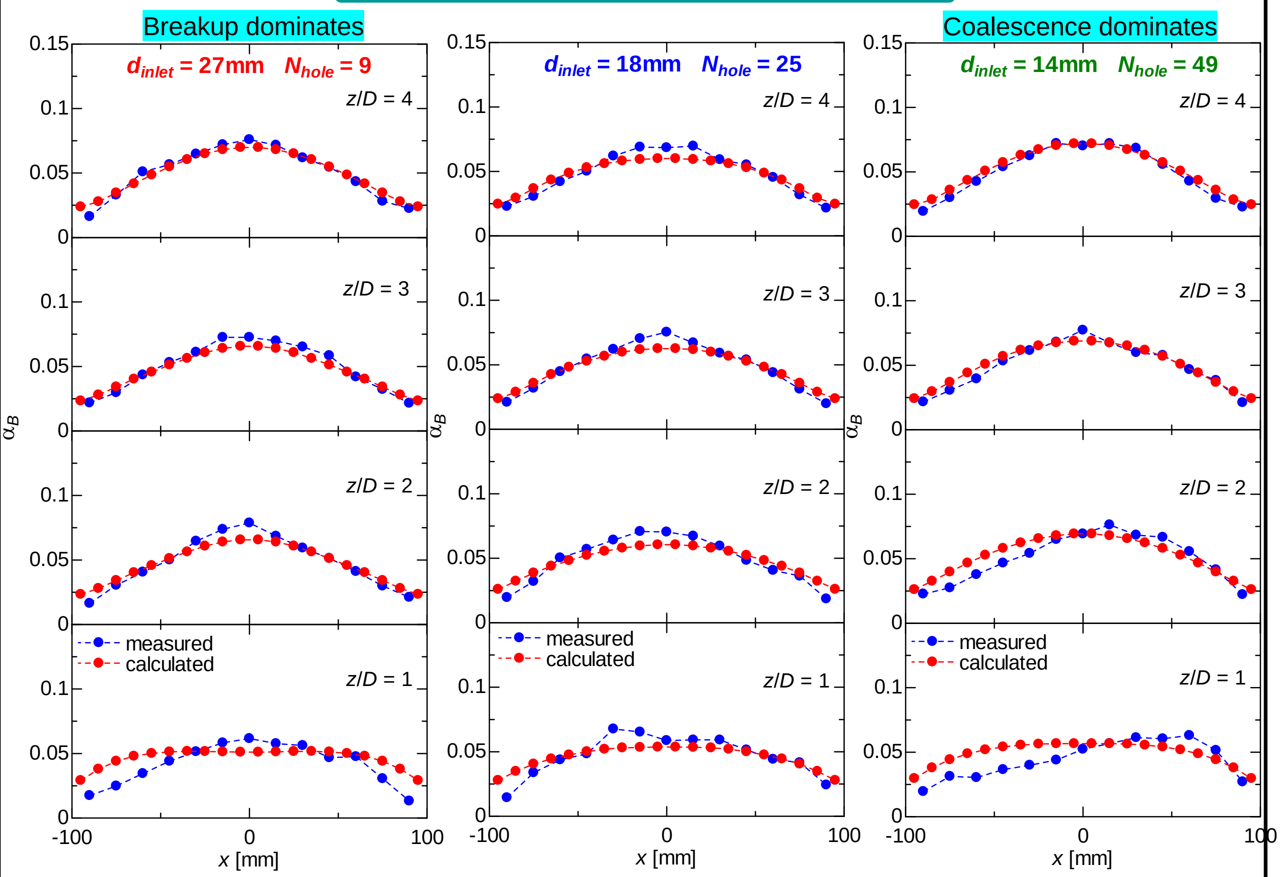

Experimental Setup and Condition

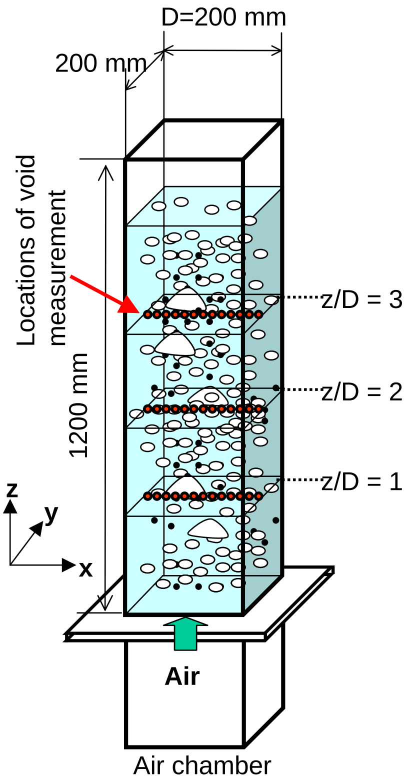

Silica particle: d=60, 100, 150 μm,
ρ=1320kg/m³
hydrophilic, spherical

Particle concentration C_S : 0, 20, 40 vol.%

Gas volume flux J_G: 0.02, 0.034 m/s

Inlet bubble diameter: 10.9, 12.6 mm

Initial water level: 1 m

Void distribution: Conductivity probe

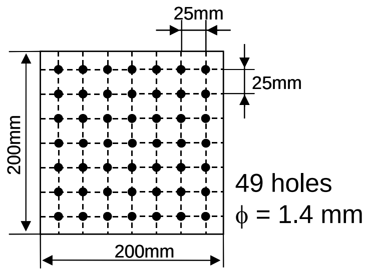

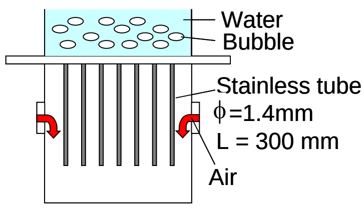

Effect of Particles on Flow Patterns

J_G = 0.02 m/s d_S = 100 μm J_G = 0.034 m/s

C_S = 0 % 20 % 40 % C_S = 0 % 20 % 40 %

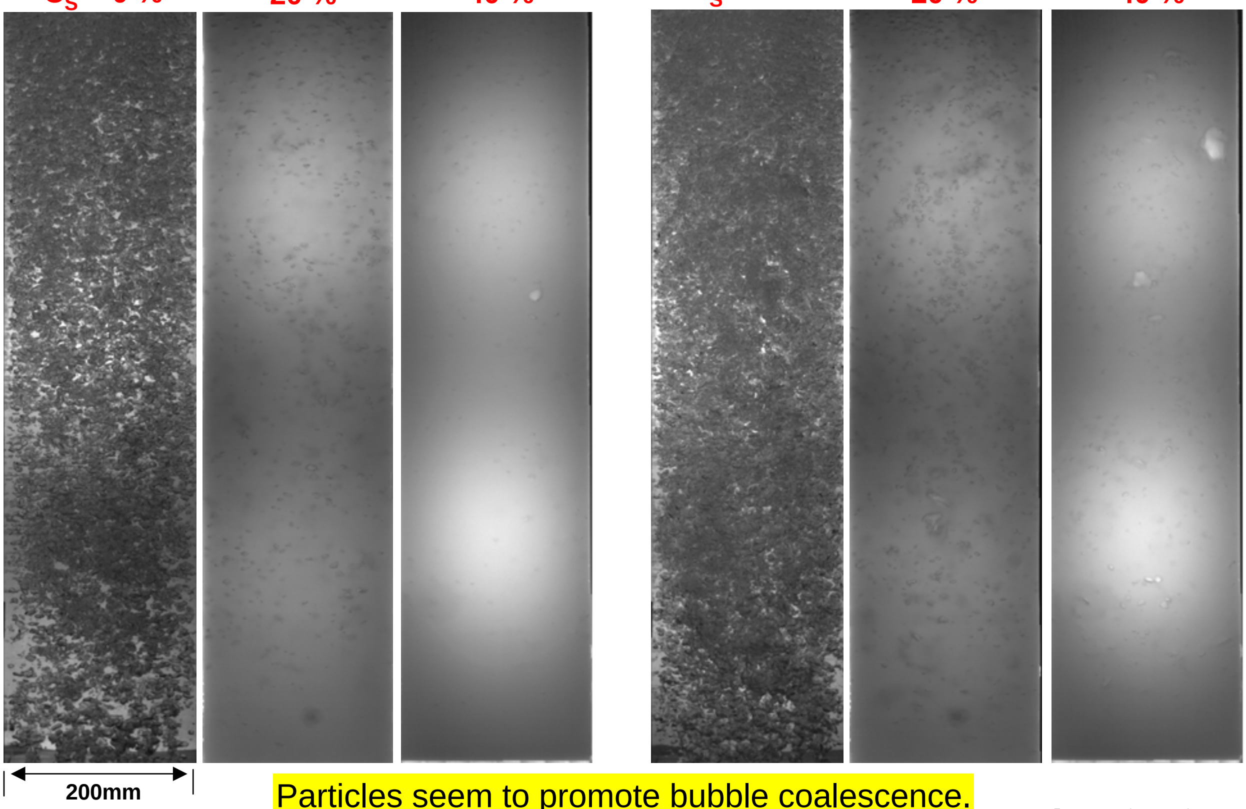

Particles seem to promote bubble coalescence.

Effects of Particle Concentration on Void Distributions

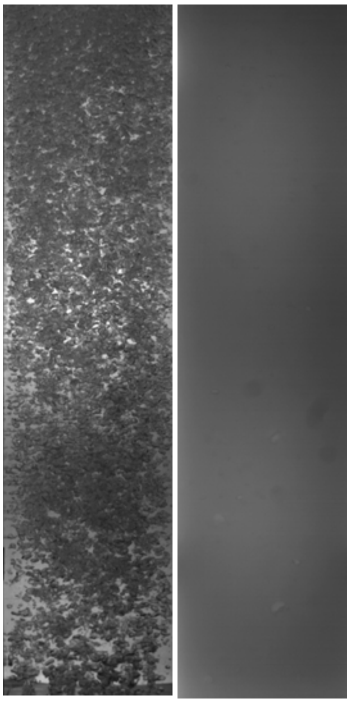

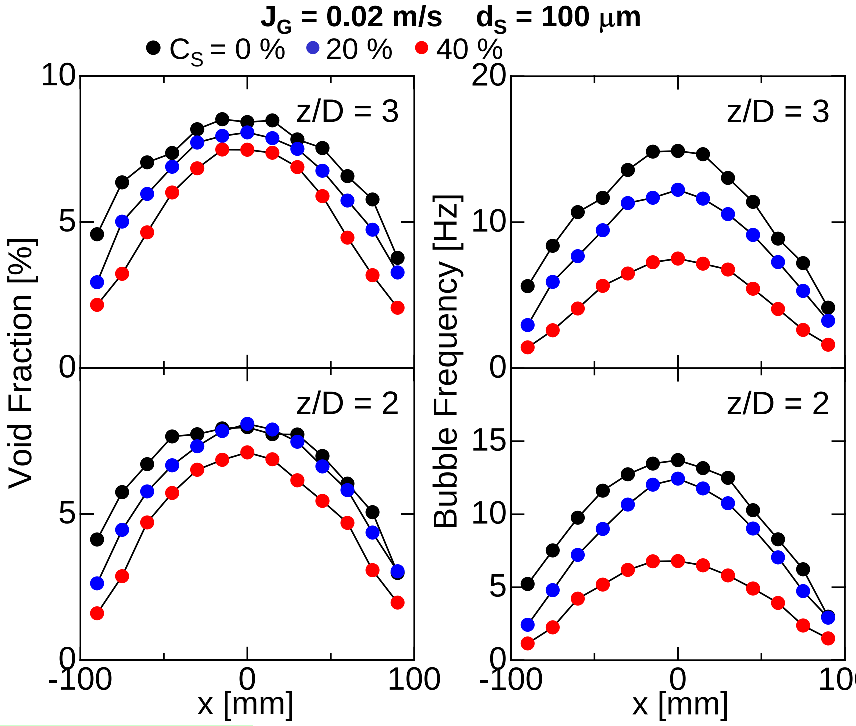

Void fraction decreases with increasing C_S.
➡ Bubble velocity increases with C_S.

Number of bubbles decreases with increasing C_S.
➡ Particles promote coalescence.

Observation of Particle Effects

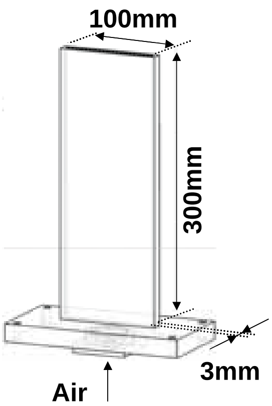

Bubble in narrow parallel plates

d_S = 100 μm

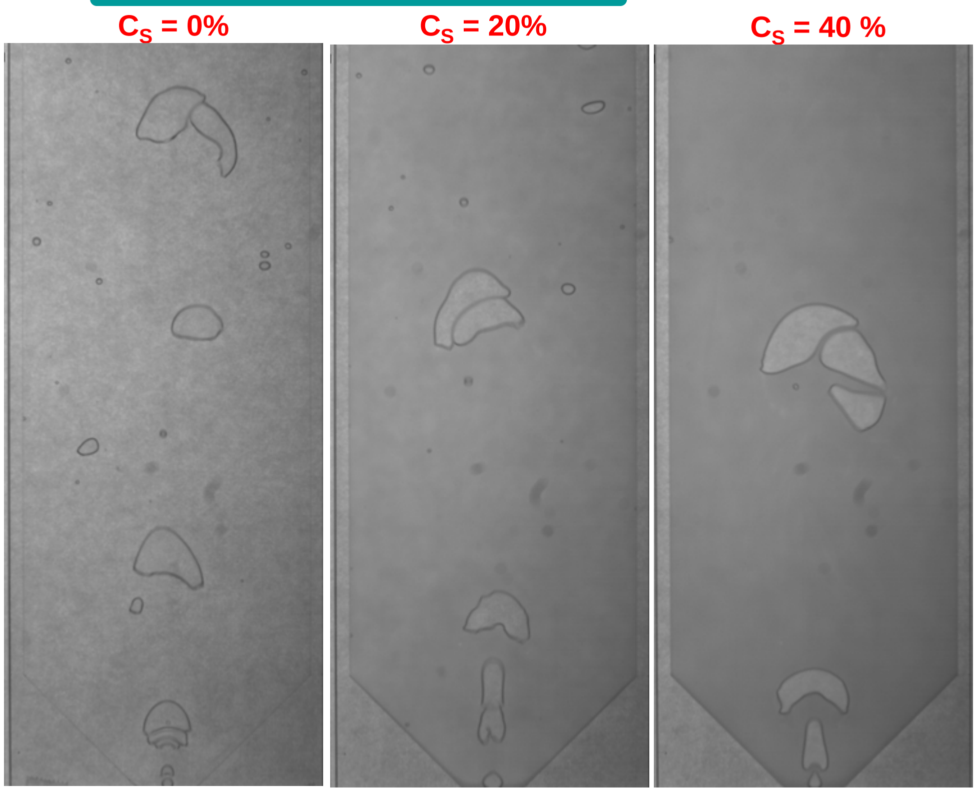

"Time required for coalescence" decreases with increasing C_S.
➡ Increase in coalescence probability

Measurement of Time required for Coalescence t_C

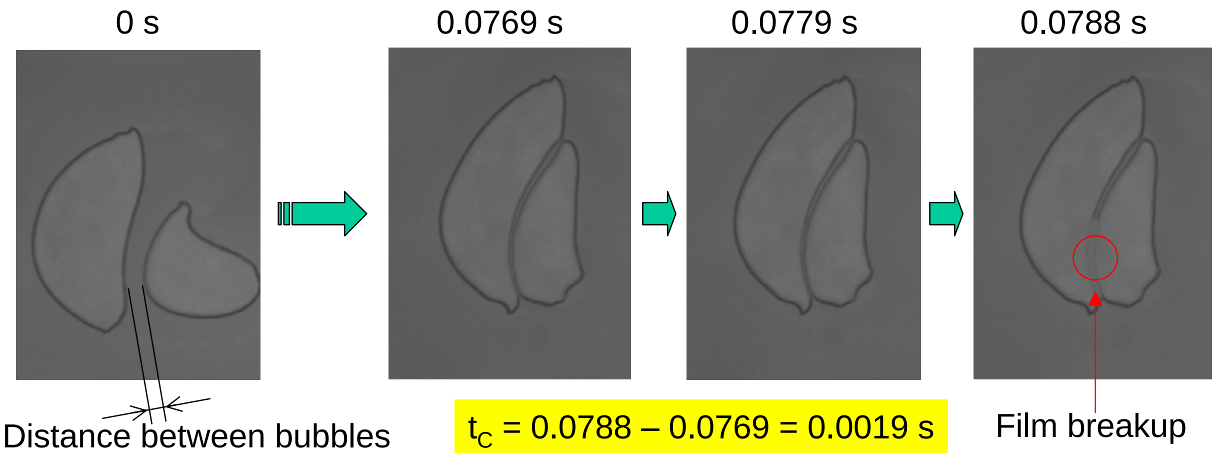

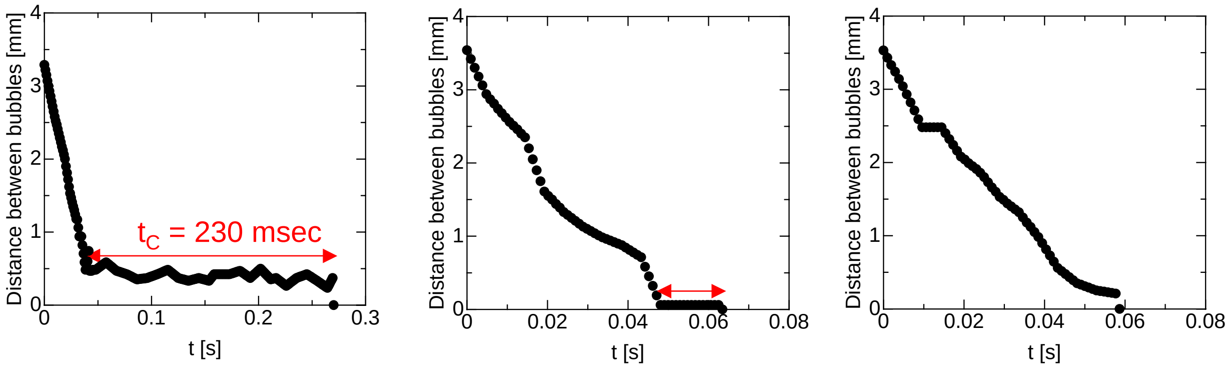

(a) Long contact: t_C = 230 msec (b) Short contact: t_C = 15 msec (c) Instantaneous coales. t_C = 0

Effect of Particle Size & Concentration on t_C

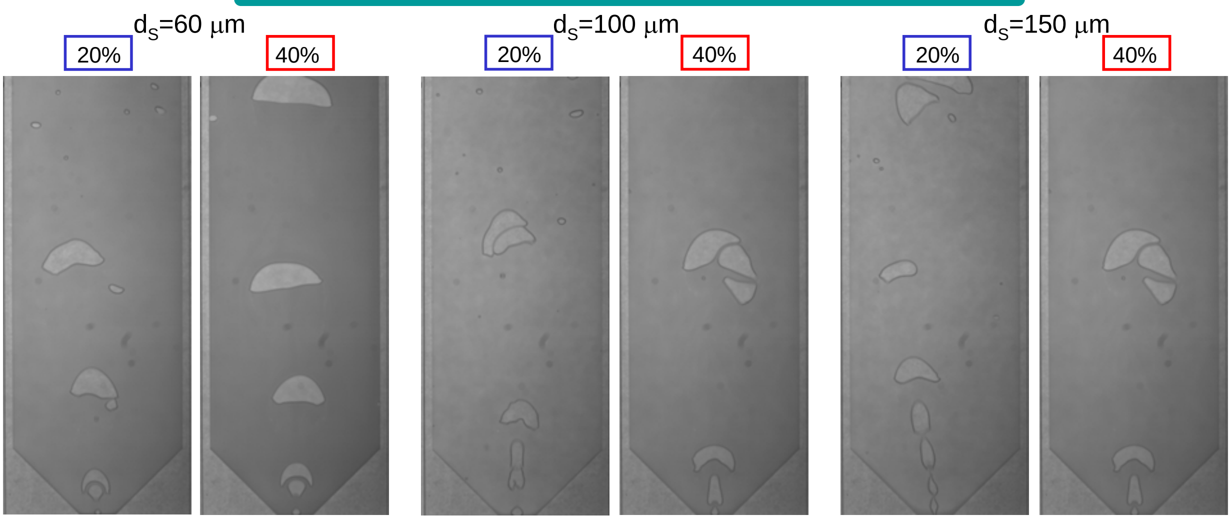

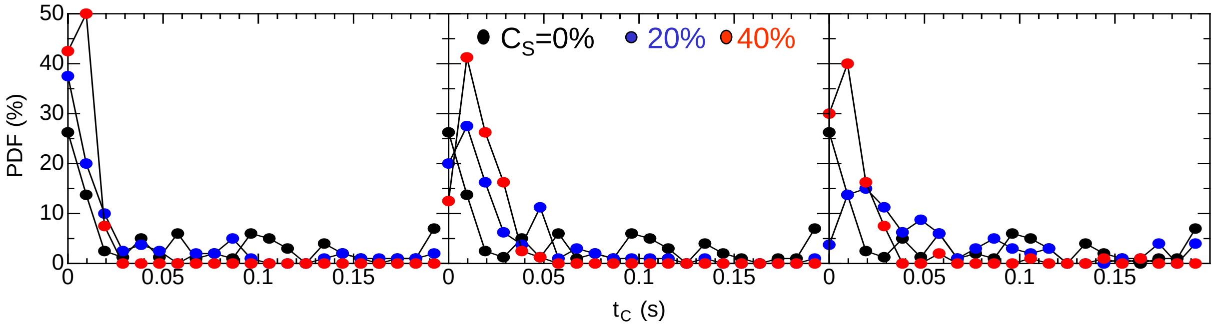

Coalescence probability increases with decreasing d_S and increasing C_S.

Introduction of a Particle Effect Multiplier to t_C

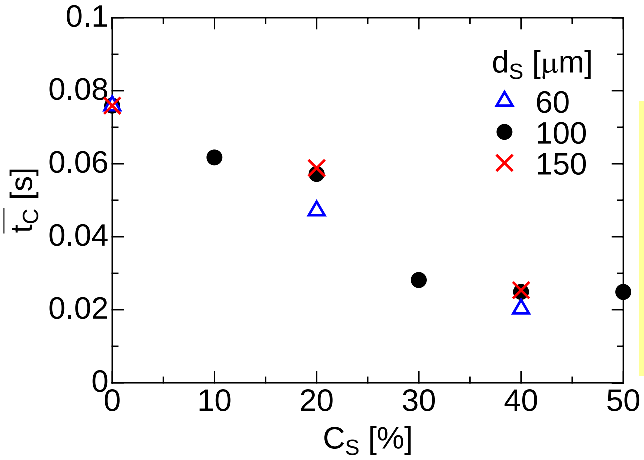

t_C decreases with increasing C_S.

t_C decreases with d_S.

t_C reaches a minimum value at C_S=40%.

Instantaneous coalescence

Coalescence efficiency: $P_C = \exp(-\beta t_C / \tau)$

β: particle effect multiplier

τ: contact time

β=1 at C_S = 0% (Gas-liquid)
β=0 for C_S > 40% (Instantaneous coalescence)
β~0.5 at C_S = 20% (Experimental data)

Comparison for C_S = 0 %

J_G = 0.02 m/s
β = 1

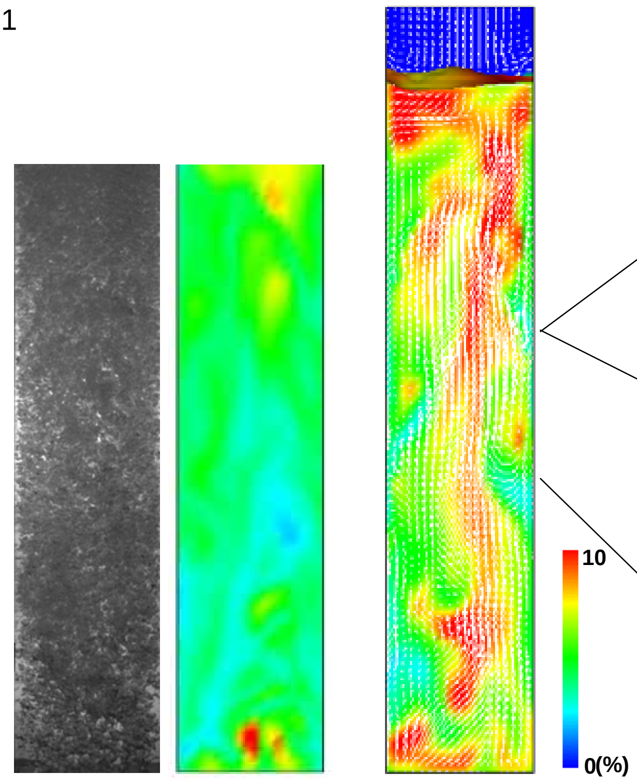

Void Fraction near the wall

Void Fraction on the center plane

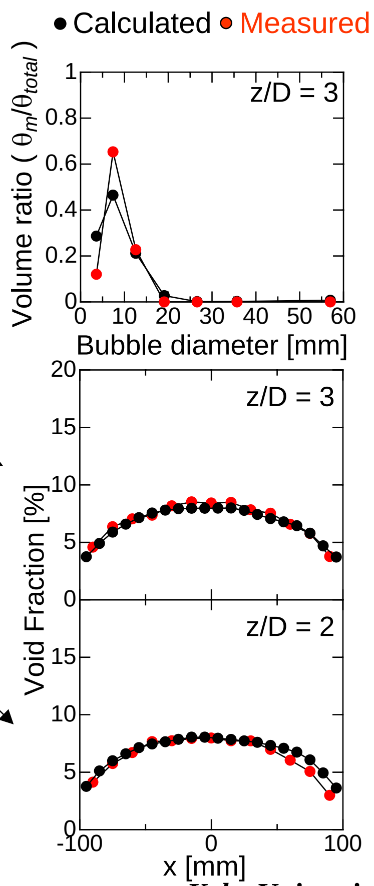

Comparison for C_S = 20 %, d_S = 100 μm

J_G = 0.02 m/s
β = 0.5

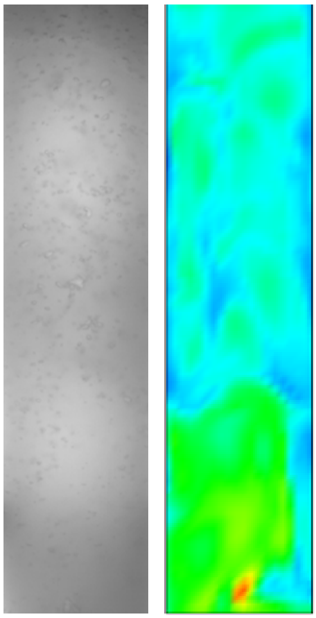

Void Fraction
near the wall

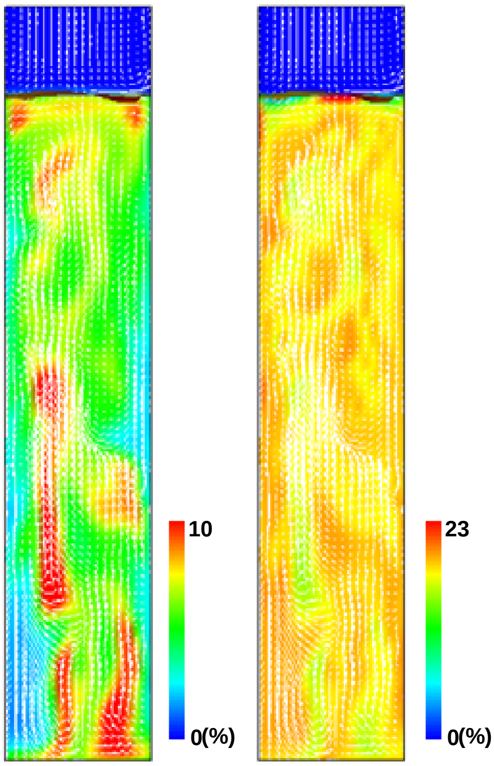

Void Fraction Particle Fraction
on the center plane

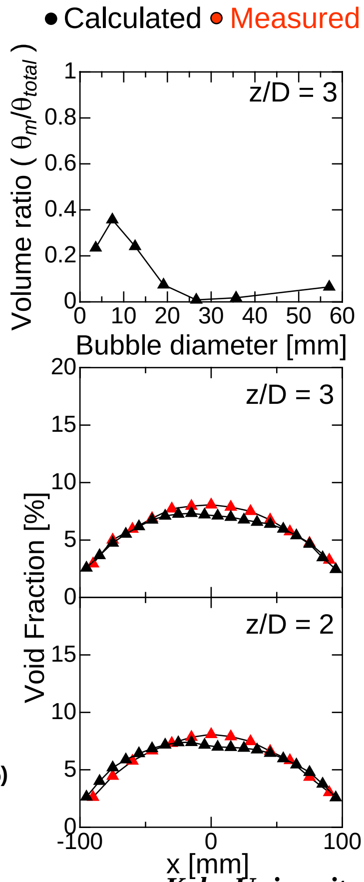

Comparison for C_S = 40 %, d_S = 100 μm

J_G = 0.02 m/s
β = 0

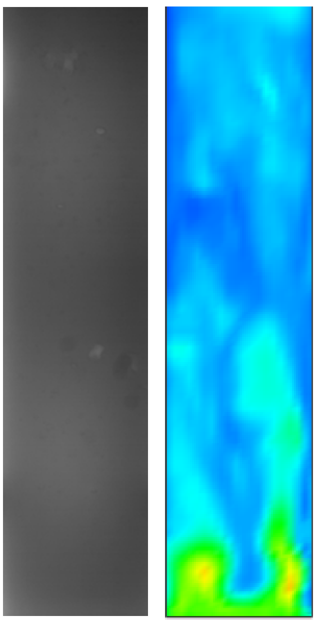

Void Fraction
near the wall

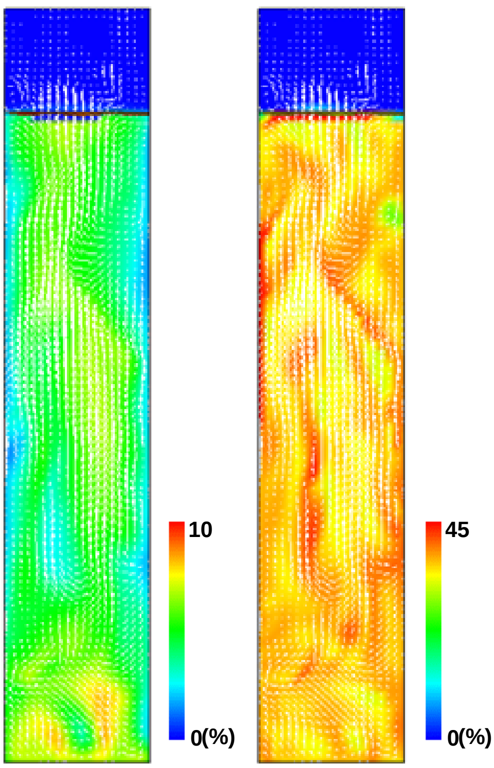

Void Fraction Particle Fraction
on the center plane

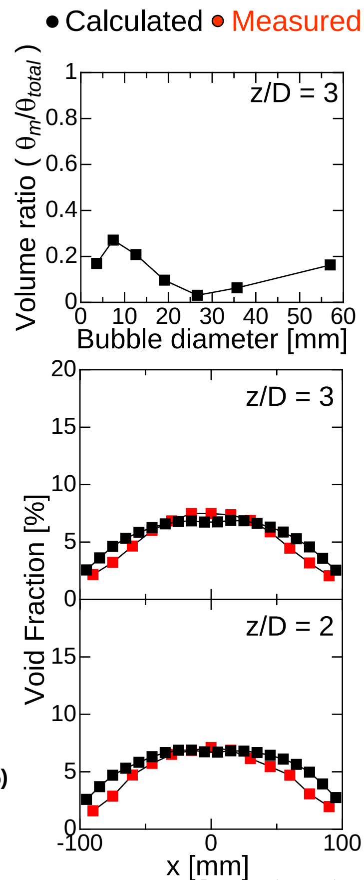

Summary

Accurate interface tracking simulation of contaminated bubbles and drops for a wide range of fluid properties and Reynolds number is possible, provided that physical properties for the adsorption and desorption kinetics are available.

Interface tracking simulation of mass transfer from a bubble for a wide range of Sc and Re numbers is also feasible, provided that HPCs are available.

Fine particles promote bubble coalescence and the effects of particles can be reasonably predicted by introducing a multiplier to the time required for coalescence.